NeuroImage: Clinical 17 (2018) 873–881

Contents lists available at ScienceDirect

NeuroImage: Clinical

journal homepage: www.elsevier.com/locate/ynicl

Brain functional connectivity in sleep-related hypermotor epilepsy

Stefania Evangelisti[a,b,1], Claudia Testa[a,b,c,1], Lorenzo Ferri[b,d], Laura Ludovica Gramegna[a,b], David Neil Manners[a,b], Giovanni Rizzo[b,d], Daniel Remondini[c,e], Gastone Castellani[c,e], Ilaria Naldi[b,d], Francesca Bisulli[b,d], Caterina Tonon[a,b], Paolo Tinuper[b,d], Raffaele Lodi[a,b,*]

[a] Functional MR Unit, Policlinico S.Orsola - Malpighi, via Massarenti 9, 40138, Bologna, Italy
[b] Department of Biomedical and NeuroMotor Sciences, University of Bologna, via U. Foscolo 7, 40123, Bologna, Italy
[c] INFN- National Institute of Nuclear Physics, Bologna, Italy
[d] IRCCS Institute of Neurological Sciences of Bologna, via Altura 3, 40139, Bologna, Italy
[e] Department of Physics and Astronomy, University of Bologna, Bologna, Italy

ARTICLE INFO

Keywords:
Sleep-related hypermotor epilepsy
Nocturnal frontal lobe epilepsy
Functional connectivity
Independent component analysis
Graph theory

ABSTRACT

Objectives: To evaluate functional connectivity (FC) in patients with sleep-related hypermotor epilepsy (SHE) compared to healthy controls.

Methods: Resting state fMRI was performed in 13 patients with a clinical diagnosis of SHE (age = 38.3 ± 11.8 years, 6 M) and 13 matched healthy controls (age = 38.5 ± 10.8 years, 6 M).

Data were first analysed using probabilistic independent component analysis (ICA), then a graph theoretical approach was applied to assess topological and organizational properties at the whole brain level. We evaluated node degree (ND), betweenness centrality (BC), clustering coefficient (CC), local efficiency (LE) and global efficiency (GE). The differences between the two groups were evaluated non-parametrically.

Results: At the group level, we distinguished 16 RSNs (Resting State Networks). Patients showed a significantly higher FC in sensorimotor and thalamic regions ($p < 0.05$ corrected). Compared to controls, SHE patients showed no significant differences in network global efficiency, while ND and BC were higher in regions of the limbic system and lower in the occipital cortex, while CC and LE were higher in regions of basal ganglia and lower in limbic areas ($p < 0.05$ uncorrected).

Discussion and conclusions: The higher FC of the sensorimotor cortex and thalamus might be in agreement with the hypothesis of a peculiar excitability of the motor cortex during thalamic K-complexes. This sensorimotor-thalamic hyperconnection might be regarded as a consequence of an alteration of the arousal regulatory system in SHE. An altered topology has been found in structures like basal ganglia and limbic system, hypothesized to be involved in the pathophysiology of the disease as suggested by the dystonic-dyskinetic features and primitive behaviours observed during the seizures.

1. Introduction

Sleep-related hypermotor epilepsy (SHE), previously known as nocturnal frontal lobe epilepsy (NFLE), is a rare and peculiar form of focal epilepsy characterise by brief (< 2 min) seizures with stereotyped motor patterns, commonly "hypermotor" events, occurring predominantly during sleep (Provini et al., 1999; Provini et al., 2000; Tinuper and Lugaresi, 2002). The diagnostic criteria of SHE were recently revised during an international consensus conference (Tinuper et al., 2016). The differential diagnosis with other non-epileptic nocturnal paroxysmal events, namely parasomnias, can be a challenge (Bisulli et al., 2011; Licchetta et al., 2017; Nobili, 2007; Tinuper et al., 2011) since in SHE interictal and ictal scalp EEGs, as well as neuroradiological findings, are often unrevealing.

Hypermotor seizures were described to arise from various areas of the frontal lobe, as expected, but also from extra-frontal regions, such as more frequently in the temporal lobe, or in the insular cortex, but also in the parietal, occipital and opercular areas (Gibbs et al., 2016). Hyperkinetic automatisms and complex behaviours appear when the ictal discharge involves structures such as the cingulate, frontal and parietal regions, irrespective of its origin (Rheims et al., 2008). These observations suggest the hypothesis that the syndrome affects a broad

* Corresponding author at: Functional MR Unit, Policlinico S.Orsola – Malpighi, Department of Biomedical and NeuroMotor Sciences (DiBiNeM), University of Bologna, Via Massarenti 9, 40138 Bologna, Italy.
E-mail address: raffaele.lodi@unibo.it (R. Lodi).
[1] Contributed equally.

https://doi.org/10.1016/j.nicl.2017.12.002
Received 3 August 2017; Received in revised form 31 October 2017; Accepted 2 December 2017
Available online 06 December 2017

Table 1
Demographic and clinical data of the patients' sample.

ID	Sex	AAE (yrs)	DD (yrs)	Seizures frequency 6 months before MR scan	AE therapy at MR scan	Diagnosis of SHE	Brain structural MRI findings
1	F	18	6	Seizure-free	CBZ	Confirmed	Negative
2	M	20	1	Multiple/night	None	Confirmed	Negative
3	F	28	3	Multiple/night	None	Clinical	Negative
4	F	29	24	1–2/night	CBZ	Confirmed	Negative
5	M	35	25	Multiple/week	OXC, PHT, LCS	Confirmed	L frontal heterotopia
6	F	36	29	Monthly	CBZ	Confirmed	Negative
7	F	42	34	Multiple/month-yearly	CBZ, TPM, CLB	Confirmed	Negative
8	M	44	30	Monthly	LTG, TPM	Confirmed	Negative
9	F	45	39	Monthly	CBZ, PB	Confirmed	Negative
10	M	46	32	Monthly	None	Clinical	Negative
11	F	49	23	Weekly	CBZ	Confirmed	L frontal FCD
12	M	50	38	Seizure-free	OXC	Clinical	Negative
13	M	55	48	Multiple/night	CBZ	Confirmed	L opercular-insular FCD

AAE: age at evaluation; DD: disease duration; AE: anti-epileptic; OXC = oxcarbazepine; PHT = phenytoin; LCS = lacosamide; CBZ = carbamazepine; TPM = topiramate; CLB = clobazam; PB = phenobarbital; LTG = lamotrigine; FCD focal cortical dysplasia.

scale of cerebral domains, hinting at a network rather than a localized disturbance process (Biraben et al., 2001).

To provide valuable insights in the pathophysiology of this syndrome, we used functional MRI (fMRI) technique to investigate brain functional connectivity (FC) during resting state, i.e. in the absence of any stimulation (Biswal et al., 1995; Lowe et al., 1998). Resting state fMRI is attractive for the simplicity of the acquisitions, but, as a counterpart, the interpretation of the results can be complicated by the amount of the analytic options and different pre-processing/processing techniques that yield subtly different types of information.

ICA (Independent Component Analysis) is a data driven approach that for fMRI data gives a set of statistically independent spatial maps, grouping together temporally coherent brain regions (resting state networks, RSNs) (Beckmann et al., 2005; McKeown and Sejnowski, 1998).

A recent analytical approach for brain FC is graph theory, which models the brain as a complex network represented by a collection of nodes and edges (Bassett and Bullmore, 2009) and provides a promising tool for describing and characterizing the topological features and the organization of brain networks (Wang et al., 2010).

Both methods have already been applied to fMRI data in the most common forms of epilepsy. ICA-fMRI studies mainly found decreased functional connectivity in temporal lobe epileptic patients compared to controls (Voets et al., 2009; Zhang et al., 2009). Graph analyses have identified a less efficient brain network organization in temporal lobe epilepsy albeit with either a more regular (Wang et al., 2014) or a more random network topology in both temporal lobe and idiopathic generalized epilepsy (Liao et al., 2010; Zhang et al., 2011).

The purpose of this study was to evaluate FC in SHE patients compared to healthy controls. We firstly used the explorative and data-driven approach of ICA to determine whether resting state fMRI can detect RSNs abnormalities in SHE patients, then, in order to further explore the organization of these complex systems, we applied graph theory. To the best of our knowledge, this is the first study that attempts to highlight possible alterations in brain FC of SHE patients.

2. Materials and methods

2.1. Subjects

Thirteen SHE patients (age = 38.3 ± 11.8 years, range 18–55 years, 6 males, disease duration = 25.6 ± 14.6 years, age at onset = 12.6 ± 6.9 years) and thirteen age and sex matched healthy controls (age = 38.5 ± 10.8 years, range 19–54 years, 6 males) participated to the study.

Diagnosis of SHE was made according to the criteria recently proposed by Tinuper et al. (2016). Ten out of thirteen patients had a diagnosis of SHE confirmed by video-EEG, while three had a clinical, video-documented diagnosis. Six patients had infrequent attacks (monthly or yearly attacks), while seven patients had weekly or nightly attacks. All but two were being treated with antiepileptic drugs. Further clinical details can be found in Table 1 and in supplementary Table 2.

All the subjects gave written consent to study participation, and the study was approved by the local Ethical Committee.

2.2. Brain MRI acquisition

Acquisitions were performed with a 1.5 T GE Signa HDx 15 scanner equipped with an 8-channel head coil. All the subjects underwent a standardized MR protocol that included 9 min of resting state fMRI acquired in two consecutive runs. Subjects were instructed to lie still with their eyes closed without falling asleep, trying not to think about anything specific. The acquisition sequence was a gradient-echo echo-planar imaging (GE-EPI, TR/TE = 3000 ms/40 ms, 34 pure axial slices *per vol.*, 90 vol. *per run,* spatial resolution = 1.875 mm × 1.875 mm × 4 mm). For each run, five initial volumes were not saved to account for the MR signal equilibration.

The MR protocol also included a 3D high-resolution volumetric T1-weighted brain structural image (FSPGR, fast spoiled gradient-echo, pure axial slices, TR/TE = 12.3 ms/5.2 ms, FOV = 25.6 cm, nv = 256, 1 mm isotropic).

2.3. Data pre-processing

The data pre-processing was conducted using FSL (Jenkinson et al., 2012, Smith et al., 2004). For each subject, the two resting state runs were pre-processed separately. Functional images were corrected for slice timing and head-motion (MCFLIRT, Motion Correction FMRIB's Linear Image Registration Tool, Jenkinson et al., 2002). A spatial smoothing (gaussian kernel FWHM = 6 mm) and a high-pass temporal filter (cut-off = 100 s) were applied.

Functional images were linearly (FLIRT with BBR method, Boundary Based Registration, Greve and Fischl, 2009) registered to 3D T1-w volumetric images, and the latter were non-linearly warped to the MNI (Montreal Neurological Institute) template using FNIRT (Andersson et al., 2007) with a subsequent resample to $2 \times 2 \times 2\ mm^3$. Functional images could then be aligned to MNI space as well by combining these two transformations.

2.4. IC analysis

IC analysis was performed using a probabilistic approach as implemented in MELODIC (Multivariate Exploratory Linear Optimized Decomposition into Independent Components 3.14 FSL tool, Smith,

2004); the number of components was automatically estimated from the data.

A single-session ICA was run and the so obtained components were manually classified between signal and noise, based on knowledge of RSN patterns and of typical artifact characteristics, as described in the literature (Beckmann et al., 2005; De Luca et al., 2006; Kelly Jr et al., 2010; Griffanti et al., 2017), using a conservative approach. Data denoising was then performed by regressing out the noise signals.

Functional images were registered to the MNI template to perform a temporally concatenated group ICA. To generate subject-specific RSN maps a dual regression approach (Filippini et al., 2009) was used, feeding into the regressions all the group components. RSN maps were then averaged across the two runs of the same subject.

2.5. Groupwise variation in RSNs

Considering the exploratory nature of these analyses, we compared all the signal RSN components across groups. Voxelwise group statistical comparisons were conducted using a nonparametric bootstrap method (FSL randomise, Winkler et al., 2014), with 5000 permutations. Age and sex were added as confounding regressors. Moreover, to control for the effect of possible local structural differences, individual modulated grey matter maps were included as voxelwise confounding regressors: grey matter maps, obtained from the T1-w images with FAST (Zhang et al., 2001), were modulated by the Jacobian maps of the non-linear transformation to MNI template in order to take into account the amount of deformation.

Statistical significance was set at $p < 0.05$ FWE-corrected for multiple comparisons with TFCE (Threshold-Free Cluster Enhancement). A further correction for multiple comparisons (Bonferroni correction) was necessary to take into account the number of different components that were compared between the two groups.

Within the SHE patients group, correlations with clinical variables (disease duration and seizure frequency) were performed, with the same nonparametric bootstrap method, only for the brain areas that showed significant differences between patients and controls.

2.6. Graph theoretical analysis

A graph theoretical approach was applied to assess topological and organizational properties at the whole brain level.

Following common practice in the field, binary undirected graphs were constructed. Nodes were defined with the subject-specific brain parcellations performed by FreeSurfer (Fischl et al., 2004). In all, 85 ROIs were included, 66 within cortical regions (left and right) and 19 within subcortical (left and right, apart from the brainstem).

The mean time series of each region was evaluated by averaging the time series of all voxels within that ROI. Pearson's correlation between the time series of each pair of ROIs was calculated. We set negative correlations, i.e. negative edge weights, to zero, as the neurophysiological interpretation of these remains controversial (Buckner, 2010) and it has been shown that zero-weighting might also improve the reliability of graph theoretical measures (Chiang et al., 2014; Wang et al., 2011). The average of the correlation matrices obtained from the two scans per subject was then used for subsequent analyses.

As there is no unique standard to choose only one proper threshold to obtain binary graphs from correlation matrix, it is quite common to investigate network properties over a range of network densities (Bullmore and Bassett, 2011). We calculated brain network topology metrics over a wide (23% to 50%, with 1% increments) range of connection densities. The limits of this range were defined on the basis of small world and connection properties of our data (see supplementary material for further details). This range is comparable to other studies in literature (Chiang et al., 2014). Each value of densities sets the number of links, allowing brain graphs with the same number of links to be compared. Links with the highest correlation coefficients were selected.

A wide number of topological measures have been defined and applied to brain networks (Rubinov and Sporns, 2010). They can be classified based on the scale in global measures and in local/node-specific. They can also be classified according to the type of information they provide, such as measures of centrality, of functional segregation or of functional integration, as in the classification by Rubinov and Sporns (2010).

We evaluated node degree (ND), betweenness centrality (BC), clustering coefficient (CC), local efficiency (LE) and global efficiency (GE). We also identified hub nodes, defined as those having a central role within a network, by considering nodes with a normalized ND or BC value at least one standard deviation greater than the average of the parameter over the network (Tian et al., 2011).

In order to compare network properties between different groups of subjects over a range of density, we followed the approach, described in the study of Tian and colleagues (Tian et al., 2011), of comparing properties of the brain graphs by integrating the topological metric over the selected range of network densities. Network measures were calculated with the toolbox BCT (Brain connectivity Toolbox, Rubinov and Sporns, 2010) and the toolbox matlabBGL, within MATLAB R2010b. Comparisons between groups were performed with a nonparametric bootstrap method (FSL randomise, Winkler et al., 2014), with 10,000 permutations. Age and sex were added as a confounding regressor. Statistical significance was set at $p < 0.05$ after FWE-correction for multiple comparisons.

3. Results

Structural images were visually inspected by experts in neuroradiology (RL, CaT). Ten patients had normal scan while three showed malformation of cortical development (two focal cortical dysplasia and one left frontal heterotopia) (Table 1).

Movement in resting state data did not exceed 1 mm of displacement or 2° of rotation in any direction, in any subject.

3.1. IC analysis

At the group level, we obtained 30 components, 16 of which were RSNs (Fig. 1).

3.2. Groupwise variation in RSNs

When comparing SHE patients and controls, we observed the most extended higher FC in sensorimotor network and thalamus (RSN component n.12 in Fig. 1), as can be seen in panel A of Fig. 2. Small but significant differences in the posterior DMN (RSN component n.14 in Fig. 1, see Fig. 2B) and in visual cortex (RSN component n.15 in Fig. 1, see Fig. 2C) were also found. These differences are statistically significant and corrected for multiple comparisons at the voxel level. When taking into account the multiple comparisons issue due to the number of components we compared (i.e. 16) by applying the Bonferroni correction, we obtained a corrected threshold of $p = 0.0031$ and in this case only the differences in motor and precuneus regions within sensorimotor network survived (Table 2).

Correlations between ICA results and clinical variables lead to no significant results.

3.3. Graph theoretical analysis

None of the parameters exhibited group differences significant under full correction for multiple comparisons, but considering the exploratory nature of the present study we report $p < 0.05$ uncorrected results, with the strong caveat that false positive results are likely to have been included.

Global efficiency showed no significant differences between SHE

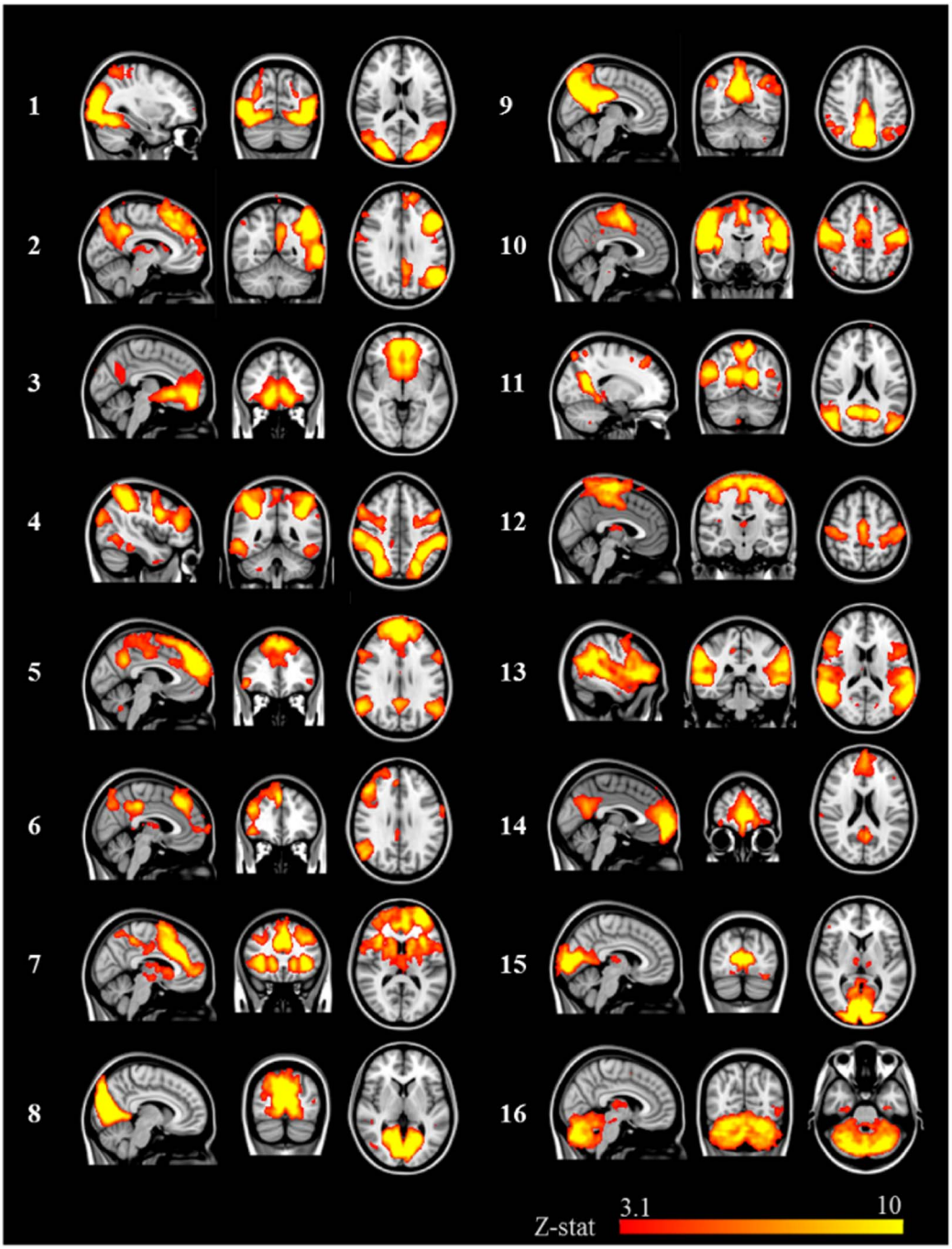

Fig. 1. Results of group level ICA: 16 RSN components; 1: visual network, 2: executive control network (left), 3: mesolimbic network, 4: dorsal attention network, 5: DMN, default mode network, 6: executive control network (right), 7: salience network, 8: visual network, 9: DMN (posterior portion), 10: sensorimotor network, 11: DMN (posterior portion), 12: sensorimotor network, 13: language network, 14: DMN, 15: visual network, 16: cerebellum and deep grey matter.

patients and healthy controls.

Local measures (i.e. node degree, betweenness centrality, clustering coefficient and local efficiency) were altered for SHE patients compared to healthy controls within the basal ganglia, limbic system, frontal lobe, visual cortex, parietal lobe, temporal lobe, brainstem and cerebellum (Table 3, Fig. 3).

A number of areas were common hubs for SHE patients and healthy controls, while some areas were hubs only for the group of patients and other areas were hubs exclusively for the group of healthy controls (Table 4, Fig. 4).

4. Discussion

In this study, we evaluated resting state FC in SHE patients using both ICA and graph theoretical approaches.

4.1. Groupwise variation in ICA RSNs

Conventional brain MRI is usually normal in sporadic and genetic forms of SHE. Thus, previous neuroimaging studies applied functional techniques to explore the autosomal dominant form of SHE (ADSHE), clinically indistinguishable from sporadic cases (Tinuper et al., 2016). Studies using PET and SPECT techniques showed altered uptake mainly within the striatum, basal ganglia, mesencephalic and frontal regions (Fedi et al., 2008; Hayman et al., 1997; Picard et al., 2006) whereas mild but widespread alteration were found in a combined study of magnetization transfer and diffusion weighted imaging (Ferini-Strambi et al., 2000).

The most relevant result in the present study is the higher FC in thalamus and sensorimotor cortex of SHE patients compared to the control group.

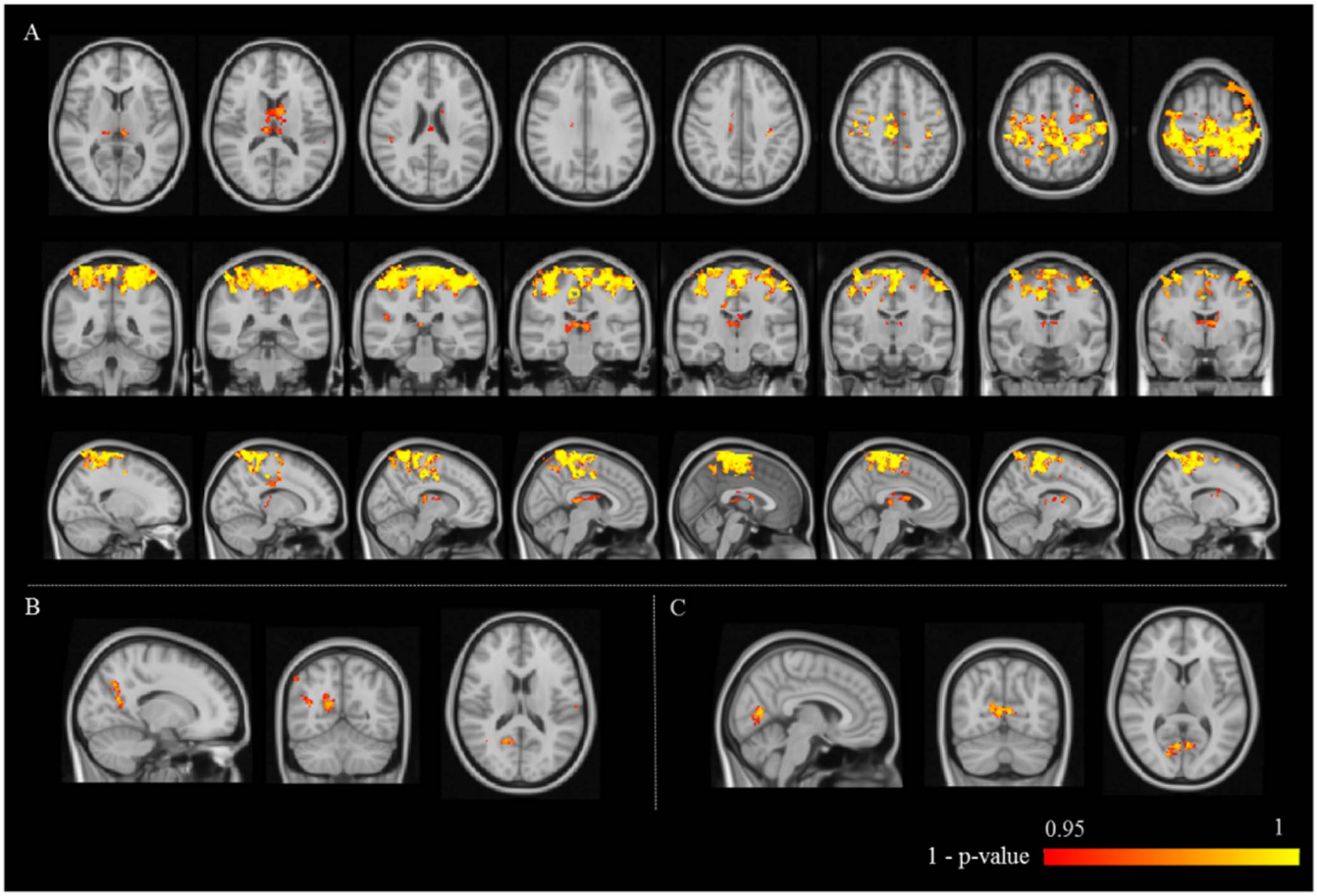

Fig. 2. ICA results: areas of increased FC in patients compared to controls within sensorimotor network (A), DMN (B) and visual network (C). Statistical maps ($p < 0.05$ corrected at the voxel level) are overlaid on the MNI-152 T1 template and shown in radiological convention.

The thalamus does not markedly show up in our group ICA sensorimotor RSN component's spatial map, and this is consistent with the fact that the thalamus is not typically considered part of the motor network. Nevertheless, when comparing the FC between the two groups, differences that are located in the thalami are found. This should not be unexpected with resting state fMRI ICA: differences in FC can be also found in brain regions that were not significantly included in the initial group spatial map of the component, as the permutation testing identifies any region where the association between the time-course of a network and the subject-specific functional signal differs among groups.

The role of the thalamus in the pathophysiology of different forms of epilepsy is well known, and previous studies have shown altered thalamic FC in temporal lobe epilepsy (Chen et al., 2015) and idiopathic generalized epilepsy (Kim et al., 2014; Masterton et al., 2012; Moeller et al., 2011). A recent EEG-fMRI study (Bagshaw et al., 2017) specifically demonstrated alterations in thalamic functional connectivity in idiopathic generalized epilepsy patients, showing a higher thalamocortical connectivity in patients. However, when thalamic functional connectivity was investigated in non-SHE frontal lobe epilepsy patients, no significant differences with healthy controls were found (Dong et al., 2016).

The alteration within motor and thalamic regions that we found in sporadic SHE is in line with the genetics of the corresponding familiar form and their common clinical and neurophysiological findings.

In ADSHE, primary genetic defects were isolated to the genes coding for the subunits of the neuronal nicotinic acetylcholine receptors (nAChRs) (Tinuper et al., 2016), and functional studies of mutant nAChRs have demonstrated their epileptogenic role in ADSHE (Marini and Guerrini, 2007).

As cholinergic neurons system modulates sleep and arousal at the level of thalamus - where mutant nAChRs present a high density (Marini and Guerrini, 2007) - and cortex, this network was linked to sleep-related disorders. Consistently, PET studies suggested a hyperactivation of the cholinergic pathway ascending from the brainstem in ADSHE patients (Picard et al., 2006).

The high prevalence of arousal disorders, parasomnias, in the personal and family histories of patients with SHE suggests a common impairment in the pathway controlling arousal in both disorders (Bisulli et al., 2010). SHE patients have more micro-arousals, and sleep-related motor attacks tend to arise during unstable sleep, with intense cyclic micro-arousal activity often occurring pseudoperiodically (Nobili et al., 2007; Parrino et al., 2006). Frequently, seizure onset corresponds to the occurrence of K-complexes generated in the thalamus, that probably provoke periodic cortical arousal (Parrino et al., 2006). This finding supports the hypothesis that thalamocortical projections may trigger the epileptic foci (Montagna et al., 1990; Tinuper and Lugaresi, 2002). K-complexes are considered an EEG epiphenomenon of an underlying mechanism that maintains the sleep state by gating external sensory information during sleep. Co-registered EEG-fMRI during spontaneous sleep showed that K-complexes correlated with bilateral increased signal in thalami, insula, precentral gyri, superior temporal gyri and in the posterior midline cortex (Caporro et al., 2012) supporting the hypothesis that K-complexes genesis is related to activity of regions beyond the thalamus, such as primary sensorimotor cortices.

Given all these observations, the altered thalamic FC in SHE patients showed in our study reflects the dysfunction of the arousal regulatory system, to date the main pathophysiological mechanism assumed in this disorder (Bisulli et al., 2010; Parrino et al., 2006; Tinuper and Lugaresi,

Table 2
ICA results: brain areas showing a significantly higher FC in SHE compared to controls within sensorimotor network (A), DMN (B) and visual network (C).

Brain Region	*p* value	Extent (mm^3)	x (mm)	y (mm)	z (mm)
A					
PostCG L	**0.0004**	21,016	− 42	− 32	54
PostCG R	**0.0004**	18,320	38	− 30	56
PreCG L	**0.0004**	19,336	− 4	− 20	58
PreCG R	**0.0004**	17,712	36	− 24	64
PC L	**0.0008**	7312	− 14	− 46	50
PC R	**0.0004**	7984	6	− 52	70
SMA L	**0.0008**	4592	− 2	− 14	58
SMA R	**0.0008**	3616	4	− 12	72
SPL L	**0.0004**	7944	− 18	− 50	62
SPL R	**0.0004**	8392	14	− 52	68
Thal L	0.0162	6818	− 6	− 26	8
Thal R	0.0188	6128	6	− 30	10
B					
AngG R	0.0350	104	42	− 58	20
PC R	0.0120	1320	18	− 60	34
CentrOp L	0.0312	64	− 60	− 20	18
C					
IntCalc L	0.0100	392	− 4	− 70	10
IntCalc R	0.0082	1584	2	− 68	12
LingG L	0.0388	168	− 10	− 64	− 2
LingG R	0.0120	224	8	− 70	4

Brain regions identification was based on the Harvard Oxford Atlas. Coordinates are in MNI space (mm). *P* values shown in bold are significant after Bonferroni correction for the number of RSNs considered. PostCG: postcentral gyrus, PreCG: precentral gyrus, PC: precuneus, SMA: supplementary motor area, SPL: superior parietal lobe, Thal: thalamus, AngG: angular gyrus, CentrOp: central operculum cortex, IntCalc: intracalcarine cortex, LingG: lingual gyrus, L: left, R: right.

2002). A higher functional connectivity is not always ascribable to a positive compensatory mechanism, it might also reflect a pathologic over-synchronization in brain activity.

The other findings of our study are the detection of higher connectivity in the precuneus and in the occipital cortex. The involvement of the precuneus is consistent with the impairment of DMN demonstrated in frontal lobe epilepsy both in adults (Cao et al., 2014) and children patients (Widjaja et al., 2013), and alterations within the occipital cortex has previously been observed with ICA in pediatric frontal lobe epilepsy (Widjaja et al., 2013).

4.2. Graph theoretical analysis

Brain functional networks present the property of small-worldness, which supports both integrated and distributed information processing and maximizes the efficiency of propagating information at a relatively low cost (Achard and Bullmore, 2007). In our study the networks were studied in a range of link densities that assured this property was maintained in the observed data.

In this regime, as for brain network organization our patients showed an unaltered global efficiency. In other forms of epilepsy, global efficiency was found to be both altered or unchanged (Liao et al., 2010; Pedersen et al., 2015; Ridley et al., 2015; Vlooswijk et al., 2011; Wang et al., 2014).

Hubs evaluation was unable to identify a hub in the caudate nucleus of SHE patients, although it is a hub for control subjects. This can be considered consistent with the impaired functionality of basal ganglia in the disorder (Fedi et al., 2008). Consistently with our ICA results, the bilateral precentral gyri and right precuneus are hubs specifically for patients.

Overall, alterations of topographical properties have been found in brain regions that are in agreement with the hypotheses about the pathophysiology of the disease and previous data from neuroimaging studies. It is unsurprising that some topological measures are either increased or decreased in different nodes of the networks, since this would be the expected outcome of an aberrant dynamic reconfiguration of functional brain. Specifically, variations of centrality graph measures as ND and BC affect the same frontal areas (pars opercularis, anterior cingulate and latero-orbital frontal cortex) suggested by the ictal semiology. Interictal PET and ictal SPECT in SHE patients showed a hypoperfusion in left frontopolar regions of one patient and hyperperfusion in right parasagittal midfrontal regions of another patient (Hayman et al., 1997). Using PET scans of acetylcholine receptor tracers and of FDG, Picard and colleagues (Picard et al., 2006) showed a lower uptake of acetylcholine in patients compared to healthy controls in the prefrontal cortex while the FDG-PET showed a reduced glucose metabolism in orbitofrontal cortex.

Higher CC and LE in caudate nucleus and globus pallidus are in line with the hypothesis that the epileptic discharge acts as a trigger for the appearance of inborn motor patterns, that the basal ganglia can contribute to the beginning of the locomotion (Tassinari et al., 2005). Functional impairment of the basal ganglia in ADSHE patients has also been showed in the form of a reduction of dopamine uptake (Fedi et al., 2008) and a lower uptake of acetylcholine receptor in the right caudate

Table 3
Whole brain graph analysis measures results.

Brain Region	ND	BC	CC	LE
Posterior cranial fossa				
Brainstem	–	–	↑	↑
Cerebellum cortex L	↓	–	–	–
Cerebellum cortex R	↓	–	–	–
Basal ganglia				
Caudate nucleus L	–	↓	↑	↑
Caudate nucleus R	–	–	↑	↑
Pallidum R	–	–	↑	↑
Frontal lobe				
Caudal middle frontal R	–	↓	–	–
Lateral orbito frontal L	–	–	↑	–
Lateral orbito frontal R	–	–	↑	–
Pars opercularis R	↑	↑	–	–
Pars triangularis L	–	↑	–	↓
Pars triangularis R	–	↑	–	↓
Precentral L	↑	–	–	–
Parietal lobe				
Superior parietal L	↑	↑	–	–
Supramarginal L	↑	–	–	–
Temporal lobe				
Fusiform R	↑	–	–	–
Transverse temporal	–	–	↓	↓
Limbic system				
Amygdala L	↑	↑	–	–
Amygdala R	–	–	–	↑
Insula R	↑	↑	–	–
Isthmus cingulate L	–	↑	–	–
Isthmus cingulate R	–	↑	–	–
Parahippocampal L	–	–	↓	↓
Parahippocampal R	–	–	–	↓
Posterior cingulate L	–	–	↑	↑
Rostral anterior cingulate L	–	–	–	↓
Rostral anterior cingulate R	–	–	↓	↓
Visual system				
Cuneus R	–	↓	↑	↑
Lateral occipital L	–	↓	↑	↑
Pericalcarine L	–	↓	↑	↑
Pericalcarine R	–	↓	↑	↑

ND: node degree, BC: betweenness centrality, CC: clustering coefficient, LE: local efficiency, ↑: higher parameter in SHE compared to healthy controls, ↓: lower parameter in SHE compared to healthy controls, −: no differences between the groups. Brain areas are grouped into posterior cranial fossa, basal ganglia, frontal lobe, parietal lobe, temporal lobe, limbic system and visual system. For brevity, only areas that showed a difference are reported (see supplementary Table 1 for the complete list of areas). P values of significant differences and median values across the groups are reported in supplementary material (supplementary Table 3).

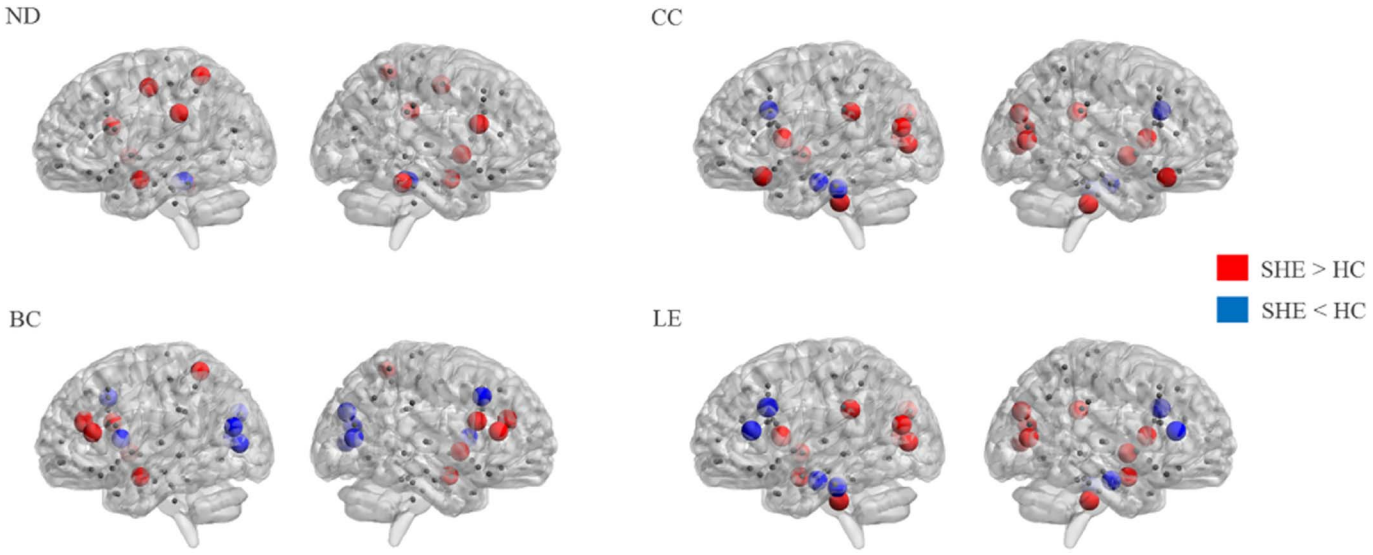

Fig. 3. Whole brain graph analysis measures results: ND, node degree; BC, betweenness centrality; CC, clustering coefficient; LE, local efficiency. Nodes where the parameter showed any differences are represented with bigger dots, in red if the parameter was higher in SHE compared to healthy control, in blue if it was lower in SHE. Left and right hemispheres are shown on the left and on the right respectively.

Table 4
Results of whole brain graph analysis hub evaluation.

Common hubs in SHE and HC	Hubs in SHE only	Hubs in HC only
Cerebellum cortex R	Fusiform R	Caudate nucleus L and R
Fusiform L	Insula R	Cerebellum cortex L
Hippocampus L and R	Precentral L and R	Lingual L
Insula L	Precuneus R	
Lateral orbito frontal L	Superior parietal L and R	
Middle temporal R	Supramarginal L	
Posterior cingulate L and R		
Superior frontal L and R		
Superior temporal L and R		
Ventral DC L and R		

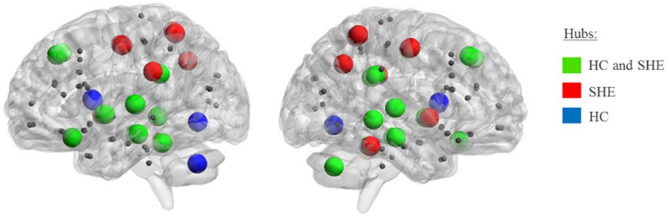

Fig. 4. Whole brain graph analysis: hub evaluation. Nodes coloured in green are hubs for both healthy controls and SHE patients, nodes in red are hubs exclusively for SHE patients, while nodes in blue are hubs only for the healthy subjects.

(Picard et al., 2006). Alterations of connections between basal ganglia (specifically caudate nucleus, globus pallidus and putamen) and both limbic and frontal areas were also described in non-SHE frontal lobe epilepsy patients, when functional connectivity itself, and not network organization, was explored (Dong et al., 2016).

For focal epilepsy patients, network measures have also been used to describe the lateralization of alterations (Ridley et al., 2015). A large cohort of patients with well-defined epileptic foci is crucial for this type of evaluation. For SHE patients, without invasive EEG recording, the localization of the epileptogenic zone and its lateralization is often not straightforward.

For all the FC alterations discussed in the present study, it is not possible to state whether the affected areas are related to the epileptogenic zone per se or to the cumulative damage due to the chronic epileptic activity.

Some limitations of our study should be acknowledged. The number of cases is relatively small for a neuroimaging study, thus further investigations of resting state FC will be necessary to corroborate these findings. However, SHE is a rare disease (estimated prevalence in the Emilia-Romagna region of Italy: 1.8–1.9 per 100,000 residents, Vignatelli et al., 2015). Moreover, a simultaneous EEG-fMRI registration was not performed, but the resting state acquisitions were performed during the interictal period and scalp interictal EEG is typically normal in this disorder. In order to minimize the risk of subjects falling asleep, we performed the resting state acquisitions in two distinct runs (approximately 5 min each) and interacted with the patients during the interval between them. However, in the clinical history of our SHE population the risk of falling asleep in relaxing condition was not referred, consistently with the absence of pathological level of excessive daytime sleepiness that was demonstrated in a previous study (Vignatelli et al., 2006). Therefore, the expected level of sleepiness between the two groups was the same and could not explain the alterations found in SHE patients group. In any case, further studies with EEG-fMRI co-registration will be crucial to corroborate our findings, and possibly correlating resting state fMRI and interictal EEG. Moreover, it will also be of interest to compare SHE patients with patients with non-SHE epilepsy, ideally non SHE-frontal lobe epilepsy, or with sleep disturbances such as parasomnia.

5. Conclusions

In conclusion, in this first resting state study in SHE patients we explored FC using a combined ICA and graph theory approach, in order to obtain an accurate investigation of network alterations. In recent years, in fact, the concept of epileptic networks has become widely accepted, considering the clinical manifestation of epilepsy as a consequence of pathological functional network dynamics, rather than only of the pathological alteration of a specific region (Iannotti et al., 2016).

Despite the heterogeneity in our SHE population, characterizing the core of the disease, a common substrate of functional alterations was described. We detected higher connectivity in sensorimotor and thalamic regions, which is in agreement with the hypothesis of a peculiar excitability of the motor cortex during thalamic K-complexes. The sensorimotor-thalamic hyperconnection might be regarded as a

consequence of an alteration of the arousal regulatory system. No alterations in global properties of the brain network were found, while altered topology was found within basal ganglia and limbic areas, i.e. structures hypothesized to be involved in the pathophysiology of the disease as suggested by the dystonic-dyskinetic features and primitive behaviours observed during seizures.

Appendix A. Supplementary data

Supplementary data to this article can be found online at https://doi.org/10.1016/j.nicl.2017.12.002.

References

Achard, S., Bullmore, E., 2007. Efficiency and cost of economical brain functional networks. PLoS Comput. Biol. 3 (2), e17.

Andersson, J.L.R., Jenkinson, M., Smith, S., 2007. Non-linear registration aka spatial normalisation. In: Technical Report FMRIB Technical Report TR07JA2. FMRIB Centre, Oxford.

Bagshaw, A.P., Hale, J.R., Campos, B.M., Rollings, D.T., Wilson, R.S., Alvim, M.K.M., Coan, A.C., Cendes, F., 2017. Sleep onset uncovers thalamic abnormalities in patients with idiopathic generalised epilepsy. Neuroimage Clin. 16, 52–57.

Bassett, D.S., Bullmore, E.T., 2009. Human brain networks in health and disease. Curr. Opin. Neurol. 22 (4), 340–347 (Review).

Beckmann, C.F., DeLuca, M., Devlin, J.T., Smith, S.M., 2005. Investigations into resting-state connectivity using independent component analysis. Philos. Trans. R. Soc. Lond. Ser. B Biol. Sci. 360 (1457), 1001–1013.

Biraben, A., Taussig, D., Thomas, P., Even, C., Vignal, J.P., Scarabin, J.M., Chauvel, P., 2001. Fear as the main feature of epileptic seizures. J. Neurol. Neurosurg. Psychiatry 70, 186–191.

Bisulli, F., Vignatelli, L., Naldi, I., Licchetta, L., Provini, F., Plazzi, G., Di Vito, L., Ferioli, S., Montagna, P., Tinuper, P., 2010. Increased frequency of arousal parasomnias in families with nocturnal frontal lobe epilepsy: a common mechanism? Epilepsia 51, 1852–1860.

Bisulli, F., Vignatelli, L., Provini, F., Leta, C., Lugaresi, E., Tinuper, P., 2011. Parasomnias and nocturnal frontal lobe epilepsy (NFLE): lights and shadows–controversial points in the differential diagnosis. Sleep Med. 12 (Suppl. 2), S27–S32 (Review).

Biswal, B., Yetkin, F.Z., Haughton, V.M., Hyde, J.S., 1995. Functional connectivity in the motor cortex of resting human brain using echo-planar MRI. Magn. Reson. Med. 34 (4), 537–541.

Buckner, R.L., 2010. Human functional connectivity: new tools, unresolved questions. Proc. Natl. Acad. Sci. U. S. A. 107 (24), 10769–10770.

Bullmore, E.T., Bassett, D.S., 2011. Brain graphs: graphical models of the human brain connectome. Annu. Rev. Clin. Psychol. 7, 113–140 (Review).

Cao, X., Qian, Z., Xu, Q., Shen, J., Zhang, Z., Lu, G., 2014. Altered intrinsic connectivity networks in frontal lobe epilepsy: a resting-state fMRI study. Comput. Math. Methods Med. 2014, 864979.

Caporro, M., Haneef, Z., Yeh, H.J., Lenartowicz, A., Buttinelli, C., Parvizi, J., Stern, J.M., 2012. Functional MRI of sleep spindles and K-complexes. Clin. Neurophysiol. 123 (2), 303–309.

Chen, X.M., Huang, D.H., Chen, Z.R., Ye, W., Lv, Z.X., Zheng, J.O., 2015. Temporal lobe epilepsy: decreased thalamic resting-state functional connectivity and their relationships with alertness performance. Epilepsy Behav. 44, 47–54.

Chiang, S., Stern, J.M., Engel Jr., J., Levin, H.S., Haneef, Z., 2014. Differences in graph theory functional connectivity in left and right temporal lobe epilepsy. Epilepsy Res. 108 (10), 1770–1781.

De Luca, M., Beckmann, C.F., De Stefano, N., Matthews, P.M., Smith, S.M., 2006. fMRI resting state networks define distinct modes of long-distance interactions in the human brain. NeuroImage 29, 1359–1367.

Dong, L., Wang, P., Peng, R., Jiang, S., Klugah-Brown, B., Luo, C., Yao, D., 2016. Altered basal ganglia-cortical functional connections in frontal lobe epilepsy: a resting-state fMRI study. Epilepsy Res. 128, 12–20.

Fedi, M., Berkovic, S.F., Scheffer, I.E., O'Keefe, G., Marini, C., Mulligan, R., Gong, S., Tochon-Danguy, H., Reutens, D.C., 2008. Reduced striatal D1 receptor binding in autosomal dominant nocturnal frontal lobe epilepsy. Neurology 71 (11), 795–798.

Ferini-Strambi, L., Bozzali, M., Cercignani, M., Oldani, A., Zucconi, M., Filippi, M., 2000. Magnetization transfer and diffusion-weighted imaging in nocturnal frontal lobe epilepsy. Neurology 54 (12), 2331–2333.

Filippini, N., MacIntosh, B.J., Hough, M.G., Goodwin, G.M., Frisoni, G.B., Smith, S.M., Matthews, P.M., Beckmann, C.F., Mackay, C.E., 2009. Distinct patterns of brain activity in young carriers of the APOE-ε4 allele. PNAS 106 (17), 7209–7214.

Fischl, B., van der Kouwe, A., Destrieux, C., Halgren, E., Segonne, F., Salat, D.H., Busa, E., Seidman, L.J., Goldstein, J., Kennedy, D., Caviness, V., Makris, N., Rosen, B., Dale, A.M., 2004. Automatically parcellating the human cerebral cortex. Cereb. Cortex 14, 11–22.

Gibbs, S.A., Proserpio, P., Terzaghi, M., Pigorini, A., Sarasso, S., Lo Russo, G., Tassi, L., Nobili, L., 2016. Sleep-related epileptic behaviors and non-REM-related parasomnias: insights from stereo-EEG. Sleep Med. Rev. 25, 4–20.

Greve, D.N., Fischl, B., 2009. Accurate and robust brain image alignment using boundary-based registration. NeuroImage 48 (1), 63–72.

Griffanti, L., Douaud, G., Bijsterbosch, J., Evangelisti, S., Alfaro-Almagro, F., Glasser, M.F., Duff, E.P., Fitzgibbon, S., Westphal, R., Carone, D., Beckmann, C.F., Smith, S.M., 2017. Hand classification of fMRI ICA noise components. NeuroImage 154, 188–205.

Kelly Jr., R.E., Gunning, F.M., Murphy, C.F., Morimoto, S.S., Kanellopoulos, D., Jia, Z., Lim, K.O., Hoptman, M.J., 2010. Visual inspection of independent components: defining a procedure for artifact removal from fMRI data. J. Neurosci. Methods 189 (2), 233–245.

Hayman, M., Scheffer, I.E., Chinvarun, Y., Berlangieri, S.U., Berkovic, S.F., 1997. Autosomal dominant nocturnal frontal lobe epilepsy: demonstration of focal frontal onset and intrafamilial variation. Neurology 49 (4), 969–975.

Iannotti, G.R., Grouiller, F., Centeno, M., Carmichael, D.W., Abela, E., Wiest, R., Korff, C., Seeck, M., Michel, C., Pittau, F., Vuillemoz, S., 2016. Epileptic networks are strongly connected with and without the effects of interictal discharges. Epilepsia 57 (7), 1086–1096.

Jenkinson, M., Bannister, P., Brady, J.M., Smith, S.M., 2002. Improved optimisation for the robust and accurate linear registration and motion correction of brain images. NeuroImage 17 (2), 825–841.

Jenkinson, M., Beckmann, C.F., Behrens, T.E., Woolrich, M.W., Smith, S.M., 2012. FSL. NeuroImage 62, 782–790.

Kim, J.B., Suh, S.I., Seo, W.K., Oh, K., Koh, S.B., Kim, J.H., 2014. Altered thalamocortical functional connectivity in idiopathic generalized epilepsy. Epilepsia 55 (4), 592–600.

Liao, W., Zhang, Z., Pan, Z., Mantini, D., Ding, J., Duan, X., Luo, C., Lu, G., Chen, H., 2010. Altered functional connectivity and small-world in mesial temporal lobe epilepsy. PLoS One 5 (1), e8525.

Licchetta, L., Bisulli, F., Vignatelli, V., Zenisi, C., Di Vito, L., Mostacci, B., Rinaldi, C., Trippi, I., Naldi, I., Plazzi, G., Provini, F., Tinuper, P., 2017. Sleep-related hypermotor epilepsy. Long term outcome in a large cohort. Neurology 88 (1), 70–77.

Lowe, M.J., Mock, B.J., Sorenson, J.A., 1998. Functional connectivity in single and multislice echoplanar imaging using resting-state fluctuations. NeuroImage 7 (2), 119–132.

Marini, C., Guerrini, R., 2007. The role of the nicotinic acetylcholine receptors in sleep-related epilepsy. Biochem. Pharmacol. 74, 1308–1314.

Masterton, R.A., Carney, P.W., Jackson, G.D., 2012. Cortical and thalamic resting-state functional connectivity is altered in childhood absence epilepsy. Epilepsy Res. 99 (3), 327–334.

McKeown, M.J., Sejnowski, T.J., 1998. Independent component analysis of fMRI data: examining the assumptions. Hum. Brain Mapp. 6 (5–6), 368–372.

Moeller, F., Maneshi, M., Pittau, F., Gholipour, T., Bellec, P., Dubeau, F., Grova, C., Gotman, J., 2011. Functional connectivity in patients with idiopathic generalized epilepsy. Epilepsia 52 (3), 515–522.

Montagna, P., Sforza, E., Tinuper, P., Cirignotta, F., Lugaresi, E., 1990. Paroxysmal arousals during sleep. Neurology 40 (7), 1063–1066.

Nobili, L., 2007. Nocturnal frontal lobe epilepsy and non-rapid eye movement sleep parasomnias: differences and similarities. Sleep Med. Rev. 11, 251–254.

Nobili, L., Francione, S., Mai, R., Cardinale, F., Castana, L., Tassi, L., Sartori, I., Didato, G., Citterio, A., Colombo, N., Galli, C., Lo Russo, G., Cossu, M., 2007. Surgical treatment of drug-resistant nocturnal frontal lobe epilepsy. Brain 130, 561–573.

Parrino, L., Halasz, P., Tassinari, C.A., Terzano, M.G., 2006. CAP, epilepsy and motor events during sleep: the unifying role of arousal. Sleep Med. Rev. 10, 267–285.

Pedersen, M., Omidvawnia, A.H., Walz, J.M., Jackson, G.D., 2015. Increased segregation of brain networks in focal epilepsy: an fMRI graph theory finding. Neuroimage Clin. 8, 536–542.

Picard, F., Bruel, D., Servent, D., Saba, W., Fruchart-Gaillard, C., Schöllhorn-Peyronneau, M.A., Roumenov, D., Brodtkorb, E., Zuberi, S., Gambardella, A., Steinborn, B., Hufnagel, A., Valette, H., Bottlaender, M., 2006. Alteration of the in vivo nicotinic receptor density in ADNFLE patients: a PET study. Brain 129 (Pt 8), 2047–2060.

Provini, F., Plazzi, G., Tinuper, P., Vandi, S., Lugaresi, E., Montagna, P., 1999. Nocturnal frontal lobe epilepsy. A clinical and polygraphic overview of 100 consecutive cases. Brain 122, 1017–1031.

Provini, F., Plazzi, G., Montagna, P., Lugaresi, E., 2000. The wide clinical spectrum of nocturnal frontal lobe epilepsy. Sleep Med. Rev. 4 (4), 375–386.

Rheims, S., Ryvlin, P., Scherer, C., Minotti, L., Hoffmann, D., Guenot, M., Mauguière, F., Benabid, A.L., Kahane, P., 2008. Analysis of clinical patterns and underlying epileptogenic zones of hypermotor seizures. Epilepsia 49, 2030–2040.

Ridley, B.G., Rousseau, C., Wirsich, J., Le Troter, A., Soulier, E., Confort-Gouny, S., Bartolomei, F., Ranjeva, J.P., Achard, S., Guye, M., 2015. Nodal approach reveals differential impact of lateralized focal epilepsies on hub reorganization. NeuroImage 118, 39–48.

Rubinov, M., Sporns, O., 2010. Complex network measures of brain connectivity: uses and interpretations. NeuroImage 52 (3), 1059–1069.

Smith, S.M., 2004. Probabilistic independent component analysis for functional magnetic resonance imaging. IEEE Trans. Med. Imaging 23 (2), 137–152.

Smith, S.M., Jenkinson, M., Woolrich, M.W., Beckmann, C.F., Behrens, T.E.J., Johansen-Berg, H., Bannister, P.R., De Luca, M., Drobnjak, I., Flitney, D.E., Niazy, R., Saunders, J., Vickers, J., Zhang, Y., De Stefano, N., Brady, J.M., Matthews, P.M., 2004. Advances in functional and structural MR image analysis and implementation as FSL. NeuroImage 23 (S1), 208–219.

Tassinari, C.A., Rubboli, G., Gardella, E., Cantalupo, G., Calandra-Buonaura, G., Vedovello, M., Alessandria, M., Gandini, G., Cinotti, S., Zamponi, N., Meletti, S., 2005. Central pattern generators for a common semiology in fronto-limbic seizures and in parasomnias. A neuroethologic approach. Neurol. Sci. 26 (Suppl. 3), s225–s232 (Review).

Tian, L., Wang, J., Yan, C., He, Y., 2011. Hemisphere- and gender-related differences in small-world brain networks: a resting-state functional MRI study. NeuroImage 54 (1), 191–202.

Tinuper, P., Lugaresi, E., 2002. The concept of paroxysmal nocturnal dystonia. In: Bazil,

C.W., Malow, B.A., Sammaritano, M.R. (Eds.), Sleep and Epilepsy: the Clinical Spectrum. Elsevier Science, pp. 277–282.
Tinuper, P., Bisulli, F., Provini, F., Montagna, P., Lugaresi, E., 2011. Nocturnal frontal lobe epilepsy: new pathophysiological interpretations. Sleep Med. 12 (Suppl. 2), S39–S42.
Tinuper, P., Bisulli, F., Cross, J.H., Hesdorffer, D., Kahane, P., Nobili, L., Provini, F., Scheffer, I.E., Tassi, L., Vignatelli, L., Bassetti, C., Cirignotta, F., Derry, C., Gambardella, A., Guerrini, R., Halasz, P., Licchetta, L., Mahowald, M., Manni, R., Marini, C., Mostacci, B., Naldi, I., Parrino, L., Picard, F., Pugliatti, M., Ryvlin, P., Vigevano, F., Zucconi, M., Berkovic, S., Ottman, R., 2016. Definition and diagnostic criteria of sleep-related hypermotor epilepsy (SHE). Neurology 86, 1834–1842.
Vignatelli, L., Bisulli, F., Naldi, I., Ferioli, S., Pittau, F., Provini, F., Plazzi, G., Vetrugno, R., Montagna, P., Tinuper, P., 2006. Excessive daytime sleepiness and subjective sleep quality in patients with nocturnal frontal lobe epilepsy: a case-control study. Epilepsia 47 (Suppl. 5), 73–77.
Vignatelli, L., Bisulli, F., Giovannini, G., Licchetta, L., Naldi, I., Mostacci, B., Rubboli, G., Provini, F., Tinuper, P., Meletti, S., 2015. Prevalence of nocturnal frontal lobe epilepsy in the adult population of Bologna and Modena, Emilia-Romagna region, Italy. Sleep 38 (3), 479–485.
Vlooswijk, M.C., Vaessen, M.J., Jansen, J.F., de Krom, M.C., Majoie, H.J., Hofman, P.A., Aldenkamp, A.P., Backes, W.H., 2011. Loss of network efficiency associated with cognitive decline in chronic epilepsy. Neurology 77 (10), 938–944.
Voets, N.L., Adcock, J.E., Stacey, R., Hart, Y., Carpenter, K., Matthews, P.M., Beckmann, C.F., 2009. Functional and structural changes in the memory network associated with left temporal lobe epilepsy. Hum. Brain Mapp. 30 (12), 4070–4081.
Wang, J., Zuo, X., He, Y., 2010. Graph-based network analysis of resting-state functional MRI. Front. Syst. Neurosci. 4 (16).
Wang, J.H., Zuo, X.N., Gohel, S., Milham, M.P., Biswal, B.B., He, Y., 2011. Graph theoretical analysis of functional brain networks: test-retest evaluation on short- and long-term resting-state functional MRI data. PLoS One 6 (7), e21976.
Wang, J., Qiu, S., Xu, Y., Liu, Z., Wen, X., Hu, X., Zhang, R., Li, M., Wang, W., Huang, R., 2014. Graph theoretical analysis reveals disrupted topological properties of whole brain functional networks in temporal lobe epilepsy. Clin. Neurophysiol. 125 (9), 1744–1756.
Widjaja, E., Zamyadi, M., Raybaud, C., Snead, O.C., Smith, M.L., 2013. Abnormal functional network connectivity among resting-state networks in children with frontal lobe epilepsy. AJNR Am. J. Neuroradiol. 34 (12), 2386–2392.
Winkler, A.M., Ridgway, G.R., Webster, M.A., Smith, S.M., Nichols, T.E., 2014. Permutation inference for the general linear model. NeuroImage 92, 381–397.
Zhang, Y., Brady, M., Smith, S., 2001. Segmentation of brain MR images through a hidden Markov random field model and the expectation-maximization algorithm. IEEE Trans. Med. Imaging 20 (1), 45–57.
Zhang, Z., Lu, G., Zhong, Y., Tan, Q., Liao, W., Chen, Z., Shi, J., Liu, Y., 2009. Impaired perceptual networks in temporal lobe epilepsy revealed by resting fMRI. J. Neurol. 256 (10), 1705–1713.
Zhang, Z., Liao, W., Chen, H., Mantini, D., Ding, J.R., Xu, Q., Wang, Z., Yuan, C., Chen, G., Jiao, Q., Lu, G., 2011. Altered functional-structural coupling of large-scale brain networks in idiopathic generalized epilepsy. Brain 134, 2912–2928.